



UNITED NATIONS
UNIVERSITY

UNU-GTP

Geothermal Training Programme

Orkustofnun, Grensasvegur 9,
IS-108 Reykjavik, Iceland

Reports 2015
Number 6

TEM AND MT RESISTIVITY SURVEYING: DATA ACQUISITION, PROCESSING AND 1D INVERSION WITH AN EXAMPLE FROM HÁGÖNGUR GEOTHERMAL FIELD, MID-ICELAND

Ali Soumail Abdou

Geological Bureau of Comoros

CEFADER-Mde

COMOROS

abdousoumail@gmail.com

ABSTRACT

Geophysical methods are some of the most effective geothermal exploration methods. Some of them are aimed at parameters that are directly influenced by the geothermal activity, such as resistivity and thermal methods, while others are aimed at geological parameters, and thus referred to as indirect methods. Electrical resistivity methods like magnetotellurics (MT) and transient electromagnetics (TEM) are most successful in identifying geothermal resources. This report discusses these two methods and describes the data acquisition, processing and 1D inversion using a practical example from MT and TEM surveys that were carried out in the Hágöngur area, Mid-Iceland by Iceland GeoSurvey (ÍSOR), in 2011 and 2013. The data were processed and inverted one-dimensionally (1D) using different software like: SSMT2000, MTeditor, TEMX and TEMTD. The results of the 1D joint inversion are presented as resistivity cross-sections and iso-resistivity maps down to different depths. Finally, the geothermal significance of the resistivity model is discussed.

1. INTRODUCTION

Resistivity methods show the variations of resistivity in the subsurface. The use of these methods has accompanied the exploration of geothermal energy, because low-resistivity rocks have always been regarded as a good indicator of the presence of a geothermal reservoir. The experience gained in recent years has shown that the objective is not only to look for conductive bodies corresponding to the clay cap of the reservoir, but also the underlying resistive bodies in basaltic areas that can be associated more directly with the reservoir. Electrical resistivity depends on porosity and the pore structure of the rock, the salinity of the water, temperature, water-rock interaction and alteration, amount of water (saturation), pressure, and steam content in the water.

The most important resistivity methods are magnetotellurics (MT) and transient electromagnetics (TEM). These two methods, MT and TEM, are often used in conjunction since they complement each other. The first one is a passive electromagnetic (EM) exploration method that measures the orthogonal components of the electric and magnetic field at the surface of the Earth. The naturally generated variations in Earth's magnetic field are the source field, providing a wide and continuous spectrum of

EM field waves that induce currents within the earth. The second one is an active EM method that measures the EM response from eddy currents within the earth induced by a current in a loop or grounded wires on the surface.

The Hágöngur high-temperature geothermal area in Mid-Iceland is one of the 25-30 high-temperature geothermal areas in Iceland. The area is within the central volcanic zone in Iceland, a few kilometres from the western edge of Vatnajökull glacier. Belonging to the central highlands, at an elevation of about 800 m a.s.l., the area is far from habitation and very remote.

In order to establish a fuller knowledge and understanding of the internal geothermal structure of the area, several exploration surveys have been done using different methods such as the resistivity method which is discussed in this report.

An overview of the resistivity of rocks and the theoretical basis of resistivity methods, the magnetotelluric and the transient electromagnetic method is given. This is followed by a description of data acquisition, processing and interpretation of TEM and MT data from Hágöngur area. The static shift problem, skin depth of MT, and the 1D joint inversion of TEM and MT data are also discussed in some details.

2. RESISTIVITY METHODS IN GEOTHERMAL EXPLORATION

It has been proven that resistivity is one of the most useful geophysical parameter in geothermal exploration. Some of the most important factors affecting resistivity in geothermal systems are salinity, temperature, permeability and alteration. A correlation exists between these parameters and the reservoir (Hersir and Arnason, 2009; Flóvenz et al., 2012). The resistivity structure of geothermal systems is imaged better by inverting jointly MT and TEM data.

2.1 Resistivity of rocks

2.1.1 Specific resistivity

Electrical resistivity of a material is usually symbolized by the Greek letter ρ (Ωm). It is an intrinsic property of a given material which shows how strongly the material can oppose the flow of an electric current. By transmitting a current I (A) through a material of length l (m) and measure the potential difference ΔV (V) between the two sides (Figure 1), one can define the resistivity as:

$$\rho = \frac{\Delta V A}{I l} \quad (1)$$

where A is the cross-sectional area of the conducting medium (m^2).

For a material which has a cross-sectional area 1 m^2 and is 1 m long, the resistivity is defined as:

$$\rho = \frac{\Delta V}{I} \quad (2)$$

The resistivity ρ can also be defined in terms of the resistance R (Ω) as shown in the following equation:

$$\rho = R \frac{A}{l} \quad (3)$$

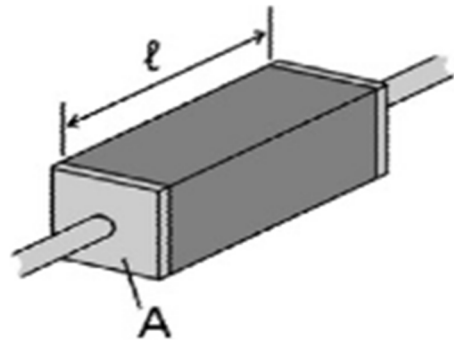


FIGURE 1: A conductive medium of cross-sectional area A and length l .

The reciprocal of resistivity is conductivity ($1/\rho=\sigma$) measured in Siemens/m.

2.1.2 Temperature

Resistivity of an aqueous solution decreases with increasing temperature, due to the increasing mobility of the ions caused by a decrease in the viscosity of the water (Figure 2). At higher temperatures, above 250°C, a change in density, viscosity and dielectric permittivity of water affects the conductivity of the ions in the solution, hence, an increase in fluid resistivity (Dakhnov, 1962). This is described by the following relationship:

$$\rho_w = \frac{\rho_{w0}}{1 + \alpha(T - T_0)} \quad (4)$$

where ρ_w = The resistivity (Ωm) of the fluid at temperature T ;
 ρ_{w0} = The resistivity (Ωm) of the fluid at temperature T_0 ;
 T_0 = The reference temperature ($^{\circ}\text{C}$);
 α = The temperature coefficient of the resistivity, $\alpha \approx 0.023^{\circ}\text{C}^{-1}$ for $T_0 = 25^{\circ}\text{C}$.

Three main conduction mechanisms are observed (Figure 3): mineral conduction which in most cases is negligible, conduction by dissolved ions in the pore fluid in geothermal which is called pore fluid conduction, and surface conduction which is the conduction caused by the (highly) mobile adsorbed ions that form a conductive layer on the surface of the pore walls.

In high-temperature geothermal systems and close to the solidus of the rock, the conductivity of the rock matrix becomes significant. The matrix conductivity follows the Arrhenius formula (see e.g. Flóvenz et al., 2012):

$$\sigma_m(T) = \sigma_0 e^{-E/kT} \quad (7)$$

where σ_m = The matrix conductivity (S/m);
 σ_0 = The conductivity at infinite temperature (S/m);
 E = The activation energy (eV);
 k = The Boltzmann constant (eV/ $^{\circ}\text{K}$); and
 T = The temperature ($^{\circ}\text{K}$).

Laboratory measurements of basalts and related material over the temperature range 400-900°C give typical value of 0.80 for E and 300 for σ_m . This shows that the matrix resistivity of basaltic rock is on the order of 1000 Ωm at 400°C and decreases to 10 Ωm at 800°C. At higher temperature, partial melt will still increase the conductivity. Since temperature exceeding 400°C can be expected in the root of the geothermal systems, the matrix conductivity will have an increasing impact on the overall conductivity.

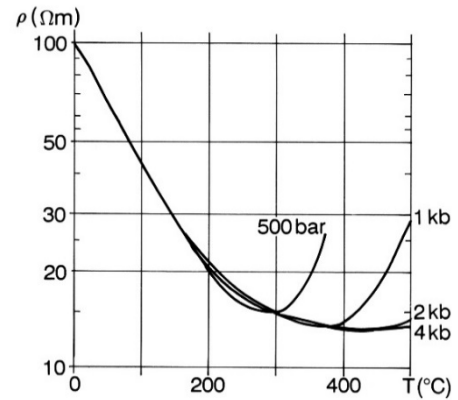


FIGURE 2: Resistivity of a NaCl solution as a function of temperature and pressure (Hersir and Björnsson, 1991; based on Quist and Marshall, 1968)

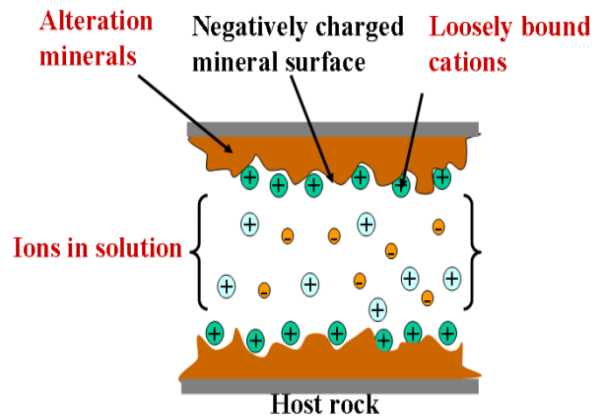


FIGURE 3: Conduction mechanisms (Hersir and Árnason, 2009)

2.1.3 Porosity

Porosity is defined as the ratio of pores to the total volume of the rock. Archie's law (Archie, 1942) has been used for relating the conductivity of a reservoir rock and the conductivity of the fluid contained in the pores. It describes the resistivity dependence on porosity if ionic conduction in the pore fluid dominates other conduction mechanisms in the rocks. For normal rocks, the law is valid only if the resistivity of the pore fluid is 2 Ωm or less and it is a very good approximation if the resistivity is dominated by that of the saturating fluid (Árnason et al., 2000). Archie's law is given by the equation:

$$\rho = \rho_w a \Phi_t^{-n} \quad (5)$$

where ρ = The bulk (measured) resistivity;
 ρ_w = The resistivity of the pore fluid (Ωm);
 a = An empirical parameter;
 Φ_t = The fractional porosity;
 n = The cementing factor.

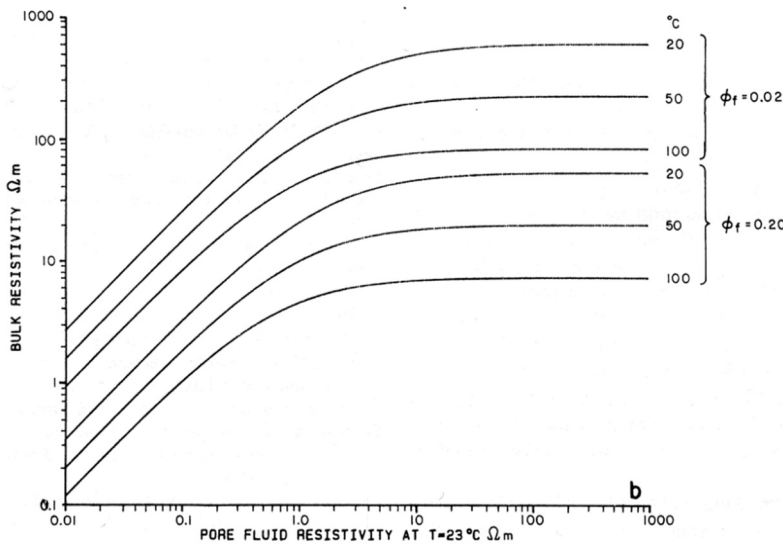


FIGURE 4: Bulk resistivity as a function of pore fluid resistivity for different pressures and porosities (Flóvenz et al., 1985)

The relationship between the bulk resistivity and the pore fluid resistivity for different porosities and temperatures for rocks in the uppermost kilometer of the Icelandic crust outside the volcanic zone is shown in Figure 4. It is based on a model put forward by Flóvenz et al. (1985). The model includes both electrolytic and surface/mineral conduction.

2.1.4 Salinity

The conductivity of the pore fluid depends on the salinity and mobility of ions present in the solution. The conductivity σ of a solution, can be determined by

considering the current flow through a cross-sectional area of 1 m^2 at a voltage of 1 V/m. It is described by the equation (Hersir and Björnsson, 1991):

$$\sigma = F \cdot (c_1 q_1 m_1 + c_2 q_2 m_2 + \dots), \quad (6)$$

where F = Faraday's number (9.649×10^4 C/mole);
 c_i = Concentration of ions;
 q_i = Valence of ions;
 m_i = Mobility of different ions.

When the amount of dissolved ions in the pore fluid increases, the conductivity also increases. Conduction in a solution is greatly affected by salinity and the mobility of ions present in the solution as shown in Figure 5.

2.1.5 Water rock interaction

Hydrothermal alteration is the interacting of hydrous (liquids), called hydrothermal fluids, reacting with surrounding rock. During the reaction, the composition of the rock is changed, through the replacing of

minerals. The interaction between hot fluids and rocks results in the formation of secondary minerals which is called geothermal alteration (Figure 6). The main factors determining which type of alteration is formed are fluid composition, permeability and temperature (Henley and Ellis, 1983). In high-temperature geothermal systems, there are relationships between alteration, subsurface resistivity, temperature and the conduction mechanism. These relationships for high-temperature geothermal systems in Iceland are shown in Figure 7 and they apply elsewhere where the host rocks are volcanic.

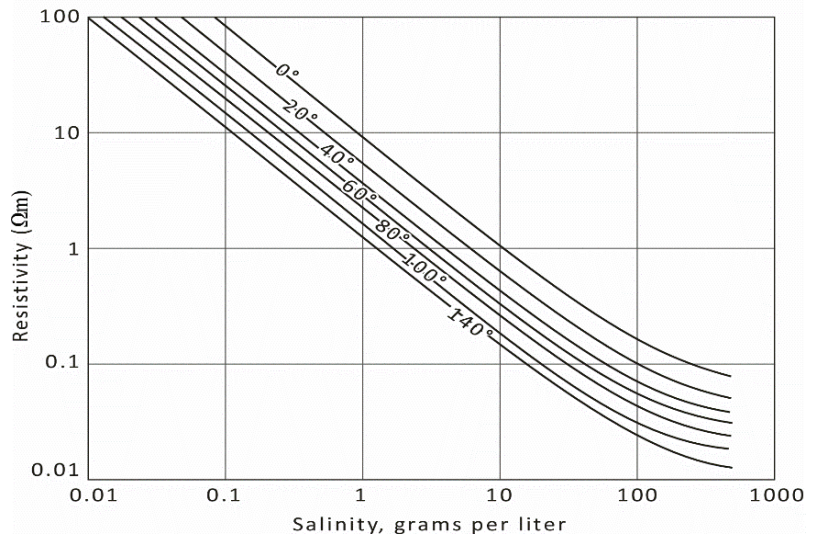


FIGURE 5: The resistivity of solutions of NaCl as a function of concentration and temperature in °C (Flóvenz et al., 2012; based on Keller and Frischknecht, 1966)

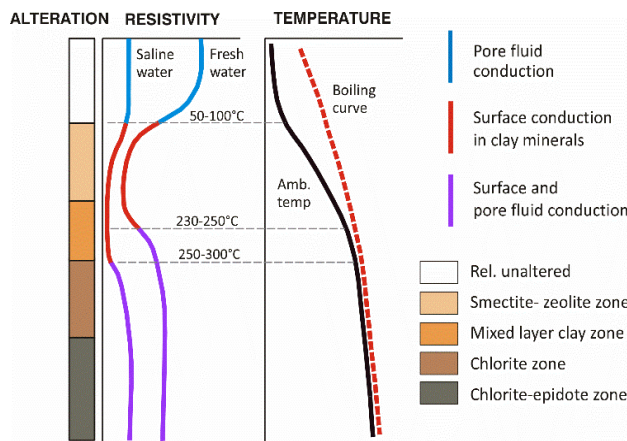


FIGURE 6: The general resistivity structure of the basaltic crust in Iceland summarized, the depth scale is arbitrary (Flóvenz et al., 2012; based on Flóvenz et al., 2005)

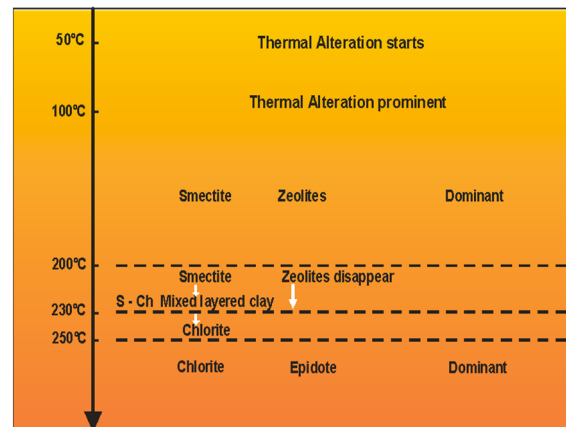


FIGURE 7: Alteration mineralogy and temperature (Hersir and Árnason, 2009)

Resistivity is high in unaltered cold formations near the surface in a typical high-temperature geothermal system. As temperature progressively increases from 50 to 100°C with depth, low-temperature mineral alterations such as smectite and zeolites are formed making the rocks conductive due to their loosely bound cations. Resistivity increases again at moderately high temperatures of about 230-240°C, where the clay minerals are gradually replaced by chlorite as the dominant alteration minerals in the transition zone of mixed-layer clays. At higher temperatures exceeding 250°C, epidote and chlorite dominate, and the system is more resistive due to the bounded ions in the crystal lattice (Árnason et al., 2010).

The subsurface resistivity structure in high-temperature geothermal fields reflects the hydrothermal alteration. The primary minerals in the host rock matrix are transformed into different minerals because of water-rock interaction and chemical transport by the geothermal fluids. Formation of alteration minerals depends on temperature and the type of primary minerals and the chemical composition of the geothermal fluid. If the alteration and temperature are in equilibrium, the subsurface resistivity structure

reflects not only the alteration but can also predict which temperature to expect. This was an important result because if the temperature that produced the alteration mineralogy still prevails, the resistivity structure can be used to predict temperature. But if cooling occurs, the alteration remains and so does the resistivity structure.

2.2 Magnetotelluric method (MT)

The magnetotelluric (MT) method is a passive geophysical prospecting method. Its principle is based on the induction of electromagnetic waves in the subsurface. The MT data acquisition requires the recording of two fields; the electric field and the magnetic field. The recording is done continuously in the time domain. The electric field data are recorded using four non-polarizable electrodes, two perpendicular dipoles. The recording of the magnetic field is done using magnetometers/coils recording two or even three orthogonal components of the magnetic field (Figure 8). The method provides information on the distribution of electrical conductivities in the underground rocks.

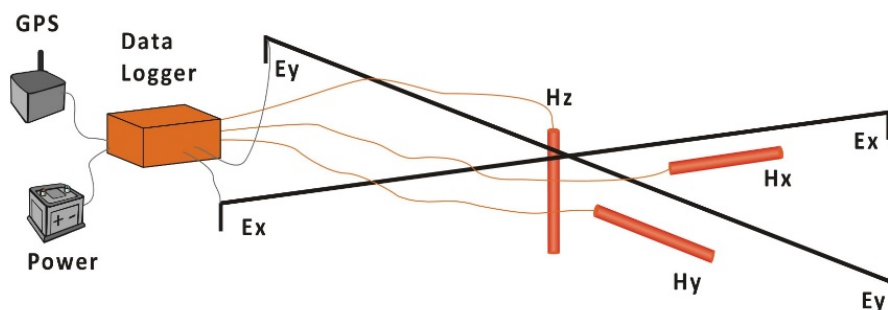


FIGURE 8: Magnetotelluric set up for data acquisition
(Flóvenz et al., 2012)

There are two sources which give rise to the MT signal:

1. At low frequencies, less than one cycle per second, the source of the signal originates from the interaction between the charged particles in the solar wind and the earth's magnetosphere and particles in the ionosphere.
2. Electromagnetic fields which have frequencies higher than 1 Hz originate from meteorological activities such as lightning discharges.

The magnetotelluric method was developed by Tikhonov (1950) and Cagniard (1953).

2.2.1 Principles

The phenomenon of electromagnetic induction is explained through Maxwell's equations. These equations describe the electric and the magnetic fields as a function of space and time and are given as (Kaufman and Keller, 1983):

Faraday's law:

$$\nabla \times \mathbf{E} = -\mu \frac{\partial \mathbf{H}}{\partial t} \quad (8)$$

Ampère's law:

$$\nabla \times \mathbf{H} = \mathbf{j} + \varepsilon \frac{\partial \mathbf{E}}{\partial t} \quad (9)$$

Gauss's law (magnetic field):

$$\nabla \cdot \mathbf{B} = 0 \quad (10)$$

Gauss's law (electric field):

$$\nabla \cdot \mathbf{D} = \eta \quad (11)$$

where \mathbf{E} = Electric field (V/m);
 \mathbf{B} = Magnetic induction (T);
 \mathbf{j} = Electrical current intensity (A/m²);
 μ = Magnetic permeability (H/m);
 ϵ = Electric permittivity (F/m);
 η = Electric charge density of free charges (C/m³);
 \mathbf{D} = Electric displacement (C/m²);
 \mathbf{H} = Magnetic intensity (A/m).

The fields and fluxes described in Maxwell's equations above are linked through the constitutive relationships, which for an isotropic medium are:

$$\mathbf{B} = \mu\mathbf{H}; \quad \mathbf{D} = \epsilon\mathbf{E}; \quad \mathbf{j} = \sigma\mathbf{E}.$$

A naturally occurring time varying magnetic field induces an electrical field which further induces eddy currents in the ground, measured on the surface in horizontal and orthogonal (E_x , E_y) directions. The electric fields are induced by the corresponding source magnetic fields (H_y and H_x) (Flóvenz et al., 2012); thus, by measuring variations in the magnetic and electrical field on the surface, subsurface resistivity and phase as a function of the frequency of the electromagnetic field are determined using the basic Maxwell's equations given above.

In a homogeneous and isotropic halfspace, using the constitutive relationships above and assuming harmonic time dependence of \mathbf{E} and $\mathbf{H} \sim e^{i\omega t}$, Faraday's and Ampère's laws may be rewritten as:

$$\nabla \times \mathbf{E} = -i\omega\mu\mathbf{H} \quad (12)$$

$$\nabla \times \mathbf{H} = \sigma\mathbf{E} + i\omega\epsilon\mathbf{E} \quad (13)$$

For an incident plane wave in a conductive halfspace, Snell's law gives:

$$\frac{1}{v_0} \sin \theta_i = \frac{1}{v} \sin \theta_t \quad (14)$$

where $v_0 = \frac{1}{\sqrt{\epsilon_0\mu_0}}$ and $v = \sqrt{\frac{2\omega}{\mu_0\sigma}}$ are the velocities of the incident EM wave in the air and in the halfspace, respectively; θ_i is the incidence angle to the surface; θ_t is the refraction angle into the halfspace; and σ the conductivity of the homogeneous earth.

Equation 14 can be rewritten as:

$$\sin \theta_t = \sqrt{\frac{2\omega\epsilon_0}{\sigma}} \sin \theta_i \quad (15)$$

For typical values of the relevant parameters, $\frac{2\omega\epsilon_0}{\sigma} < 10^{-3}$, therefore θ_t is close to zero and the incident waves travel vertically downwards for all angles of incidence θ_i and below the surface, $\frac{\partial}{\partial x} = \frac{\partial}{\partial y} = 0$.

By using the above assumptions and applying Maxwell's equations, this gives:

$$\begin{aligned} \frac{\partial^2 E_x}{\partial z^2} &= k^2 E_x, & \frac{\partial^2 E_y}{\partial z^2} &= k^2 E_y \\ \frac{\partial^2 H_x}{\partial z^2} &= k^2 H_x, & \frac{\partial^2 H_y}{\partial z^2} &= k^2 H_y \end{aligned} \quad (16)$$

where k is the wave propagation parameter, $k^2 = i\omega\mu(\sigma + i\omega\epsilon)$. Using the extreme values for the conductivity σ and the angular frequency ω : $\sigma \approx 1 - 10^{-4}$ S/m; and $\omega = \frac{2\pi}{T}$, $T = 10^{-4} - 10^4$ s, this gives $(\omega\epsilon)_{max} \approx 5 \cdot 10^{-5}$ or $\sigma \gg \omega\epsilon$. Then $k^2 \approx i\omega\mu\sigma$.

The general solutions to Equation 16 can be given as :

$$E_{x,y} = (A_{xy}e^{kz} + B_{xy}e^{-kz})e^{i\omega t} \quad (17)$$

$$H_x = \frac{1}{i\omega\mu} \frac{\partial E_y}{\partial z} = \frac{k}{i\omega\mu} (A_y e^{kz} - B_y e^{-kz}) e^{i\omega t} \quad (18)$$

$$H_y = -\frac{1}{i\omega\mu} \frac{\partial E_x}{\partial z} = -\frac{k}{i\omega\mu} (A_x e^{kz} - B_x e^{-kz}) e^{i\omega t}$$

where $A_{x,y}$ and $B_{x,y}$ are constant to be determined.

By assuming that as z goes to infinity, \mathbf{H} and \mathbf{E} go to zero, this gives $A_{x,y} = 0$, and Equations 17 and 18 become:

$$E_x = B_x e^{-kz} e^{i\omega t} \text{ and } E_y = B_y e^{-kz} e^{i\omega t} \quad (19)$$

$$H_x = -\frac{k}{i\omega\mu} B_y e^{-kz} e^{i\omega t} = -\frac{k}{i\omega\mu} E_y \quad (20)$$

$$H_y = \frac{k}{i\omega\mu} B_x e^{-kz} e^{i\omega t} = \frac{k}{i\omega\mu} E_x$$

The ratio of the electric and magnetic field, yields the Tikhonov-Cagniard wave impedance as:

$$Z_{xy} = \frac{E_x}{H_y} \text{ and } Z_{yx} = \frac{E_y}{H_x} \quad (21)$$

2.2.2 Impedance tensor

The impedance tensor (\mathbf{Z}) relates the orthogonal components of the horizontal electric and magnetic fields. In matrix notation this is given by:

$$\begin{bmatrix} E_x \\ E_y \end{bmatrix} = \begin{bmatrix} Z_{xx} & Z_{xy} \\ Z_{yx} & Z_{yy} \end{bmatrix} \begin{bmatrix} H_x \\ H_y \end{bmatrix} \quad (22)$$

The linear relationship of the fields can be written as:

$$\begin{aligned} E_x &= Z_{xx}H_x + Z_{xy}H_y \\ E_y &= Z_{yx}H_x + Z_{yy}H_y \end{aligned} \quad (23)$$

where the on-diagonal elements relate fields measured in the same direction whereas the off-diagonal elements relate the orthogonally measured fields.

For a homogeneous half space the diagonal elements Z_{xx} and Z_{yy} are zero and:

$$Z_{xy} = \frac{E_x}{H_y} = \sqrt{\omega\mu\rho} e^{i\pi/4} \text{ and } Z_{yx} = \frac{E_y}{H_x} = -Z_{xy} \quad (24)$$

The resistivity of a homogeneous half space is given by:

$$\rho_{xy} = \frac{1}{\omega\mu} |Z_{xy}|^2 = \rho_{yx} = \frac{1}{\omega\mu} |Z_{yx}|^2 \quad (25)$$

and

$$\theta = \frac{\pi}{4} = 45^\circ$$

1D impedance tensor

For layered (1D) earth, the conductivity σ changes only with the depth and the impedance tensor can be written as:

$$\begin{bmatrix} E_x \\ E_y \end{bmatrix} = \begin{bmatrix} 0 & Z_{xy} \\ Z_{yx} & 0 \end{bmatrix} \begin{bmatrix} H_x \\ H_y \end{bmatrix} \quad (26)$$

with $Z_{xx} = Z_{yy} = 0$ and $Z_{xy} = -Z_{yx}$

For an inhomogenous earth, the apparent resistivity and phase are defined as:

$$\rho_a = 0.2T|z|^2, \theta_a = \arg(z) \neq 45^\circ \quad (27)$$

where z is a linear function of the impedance tensor elements.

The apparent resistivity calculated from the off-diagonal elements of the impedance tensor in the two equations above are the same for a homogeneous and 1D earth. Rotating the impedance tensor for a non-1D earth will change the resistivity values of ρ_{xy} and ρ_{yx} . The rotationally invariant determinant of the impedance tensor, which is a kind of an average value of the apparent resistivity and phase, is commonly used for inversion (Badilla, 2011). The apparent resistivity and phase calculated from the determinant value of the impedance tensor is given by:

$$\rho_{det} = \frac{1}{\omega\mu} |Z_{det}|^2 = \frac{1}{\omega\mu} \left| \sqrt{Z_{xx}Z_{yy} - Z_{xy}Z_{yx}} \right|^2 ; \theta_{det} = \arg(Z_{det}) \quad (28)$$

2D impedance tensor

In a 2D earth environment, resistivity varies with depth and in one horizontal direction. The other horizontal direction has no variations in resistivity and is commonly known as the geoelectrical strike direction. MT impedance tensor data can be mathematically rotated with one axis perpendicular to the geoelectrical strike and the other axis parallel to it, by minimizing the off diagonal elements of the impedance tensor. The same case as in 1D, if $Z_{xx} = Z_{yy} = 0$, but here $Z_{xy} \neq -Z_{yx}$:

$$Z_{2D} = \begin{bmatrix} 0 & Z_{xy} \\ Z_{yx} & 0 \end{bmatrix} \quad (29)$$

Then the field can be split into two independent impedance tensor modes: **E**- and **B**-polarization. Both can be analyzed independently. Transverse Electric (TE) mode or **E**-polarization is when the electric field is parallel to the electromagnetic strike and Transverse Magnetic (TM) mode or **B**-polarization is when the magnetic field is parallel to the electromagnetic strike. The apparent resistivity can be calculated for each of the modes as:

$$\rho_{TE} = \frac{1}{\omega\mu} |Z_{TE}|^2; \rho_{TM} = \frac{1}{\omega\mu} |Z_{TM}|^2 \quad (30)$$

If neither of the horizontal axes are aligned along the geoelectrical strike, the diagonal elements of the impedance tensor remain $Z_{xx} = -Z_{yy} = Z$, and the off-diagonal elements Z_{xy} and Z_{yx} are independent values:

$$Z_{2D} = \begin{bmatrix} Z & Z_{xy} \\ Z_{yx} & -Z \end{bmatrix} \quad (31)$$

3D impedance tensor

The conductivity σ in a 3D earth case varies in all directions x , y and z . The general form of the impedance tensor is then:

$$Z_{3D} = \begin{bmatrix} Z_{xx} & Z_{xy} \\ Z_{yx} & Z_{yy} \end{bmatrix} \quad (32)$$

where $Z_{xx} \neq Z_{yy} \neq 0$ and $Z_{yx} \neq Z_{xy}$.

All the elements of the impedance tensor are non-zero for all rotations. A rotational invariant parameter called skew, S , is defined as:

$$S = \frac{|Z_{xx} + Z_{yy}|}{|Z_{xy} - Z_{yx}|} \quad (33)$$

This parameter indicates the dimensionality of the impedance tensor. It is close to zero for 1D and 2D earth, but large value of S indicates 3D earth.

Electrical strike shows the direction of the main horizontal geoelectrical/resistivity variation. It is calculated by minimizing the diagonal elements of impedance tensor. Often, the geoelectrical strike direction is the same direction as the geological fractures. To perform two-dimensional analysis of MT data, the impedance tensor should be rotated by an angle α . However, this approach implies a 90° ambiguity in the strike angle, so there is no way to distinguish between α and $(\alpha + 90^\circ)$ using only H_x and H_y . This ambiguity can be solved by using the Tipper based on measuring the vertical component of the magnetic field, H_z .

The vertical component of magnetic field H_z may be expressed as a linear combination of horizontal magnetic field components, H_x and H_y . It is given by:

$$H_z = W_{zx}H_x + W_{zy}H_y \quad (34)$$

where $[W_{zx} \ W_{zy}] = \mathbf{W}$ is the Wiese-Parkinson matrix, also known as the Tipper.

The matrix \mathbf{W} reflects the symmetry of the excess currents caused by horizontal variation of resistivity. For the 1D model, there are no induced currents in the vertical direction ($\mathbf{W}=0$). For the 2D model, the rotation of the coordinate system places x-axis in the strike direction (also known as a T-strike), by minimizing $|W_{zx}|$.

Skin depth

As can be seen from Equations 19 and 20, the electromagnetic fields decay exponentially with depth. The depth at which the electromagnetic field becomes e^{-1} of its surface value is called the skin depth. It is also called the penetration depth. In the case of homogeneous earth, the skin depth is defined by:

$$\delta = \frac{1}{2\pi} \sqrt{10\rho T} \approx 0.5\sqrt{\rho T} \text{ (km)} \quad (35)$$

where δ is the skin depth (km), ρ is the resistivity (Ωm) and T is the period (s).

As shown in the Equation 35, this depth is an increasing function of the period; by performing measurements for increasing periods, one thus obtains information on increasing depths of the subsurface.

2.2.3 Static shift problem

The MT method suffers the so called “static shift” problem which manifests itself in a frequency independent unknown multiplicative factor of the apparent resistivity or shift on log-scale. The static shift is a distortion of EM fields due to variations in near surface conductivity resulting in electrical field distortion, current distortion or topographic effects. The main cause is the accumulation of charges at resistivity boundaries causing the electrical field not to be continuous close to this boundary as shown in Figure 9. Consequently, the measured electric fields for the whole frequency range are affected by a

constant shift on a log scale. Thus this effect produces apparent resistivity curves with the correct shape but they are incorrectly located on the vertical logarithmic apparent resistivity axes. The flowing of the current in the ground with a localised resistivity anomaly can be deflected as shown in Figure 10. The causes of static shift can range widely, both where multiple processes and different structures give rise to unknown multipliers, S (shifts on log scale), of the apparent resistivity. In most cases those structures are not of great interest, but the interpretation of static shifted MT data will introduce errors in the results. Árnason et al. (2010), point out that shift multiplier 0.1 in MT data will result in conductivity models that have an order of magnitude too high conductivity and 3 times too shallow depths of boundaries.

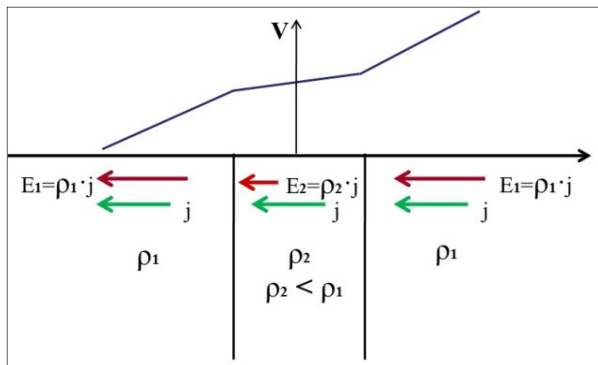


FIGURE 9: Electric field distortion causing shift (Árnason, 2015)

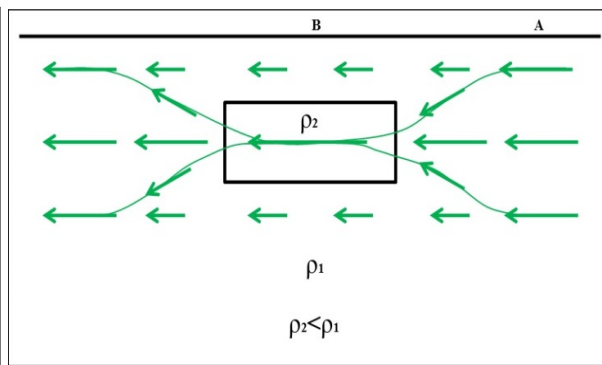


FIGURE 10: Current distortion causing static shift (Árnason, 2015)

To correct the static shift problem in MT data, the transient electromagnetics method (TEM) has been used for jointly inverting both MT and TEM data. This is based on the fact that, for TEM measurements at late time there are no distortions due to near surface inhomogeneities since they do not involve measuring the electrical field. This has been tested and shown to be a useful method to correct the static shifts in MT soundings, at least for 1D resistivity environment (Árnason, 2015).

Field example

MT soundings have been used in high-temperature geothermal fields mostly for deep prospecting. To correct for the static shift problem, ISOR developed a software for joint 1D (layered earth) inversion of MT and TEM data (Árnason, 2006a). For the data collection, TEM and MT soundings are performed in the same place within less than 200 m. The joint inversion is done for the model parameters and one additional parameter called shift multiplier, S . This multiplier is an unknown parameter by which the MT apparent resistivity values have to be divided by in order to fit the TEM data with the response of a common model as shown in Figure 11.

Figures 12 and 13 show static shift multipliers of the MT apparent resistivity derived from the determinant of the impedance tensor. The shift multipliers were determined by joint inversion with central-loop TEM soundings at the same spot (within 200 m). Figure 12 shows that half of the MT data in Hágöngur area were shifted down ($S < 1$) due to near surface conductive bodies. The static shift multiplier less than 1 shows that the apparent resistivity curve is shifted downward resulting in decreased depth to the boundaries. S higher than 1 results in higher resistivity and increased depth to the boundaries, causing an upward shift of apparent resistivity over resistive bodies (Árnason, 2015). Figure 13 shows the distribution of shift multipliers in the Hágöngur area.

2.3 Transient electromagnetic method (TEM)

The transient electromagnetics (TEM) method was developed in order to gain information on the electric resistivity of the subsurface. Unlike the magnetotelluric method, the transient electromagnetic method is an active method where a loop of wire is placed on the ground and a current is generated to run in the

loop and then suddenly terminated. The collapsing electromagnetic field induces eddy currents in the conductive underground according to Maxwell’s equations. This system of eddy currents produces a secondary magnetic field, whose propagation depends on the conductivity distribution in the subsurface (Figure 14).

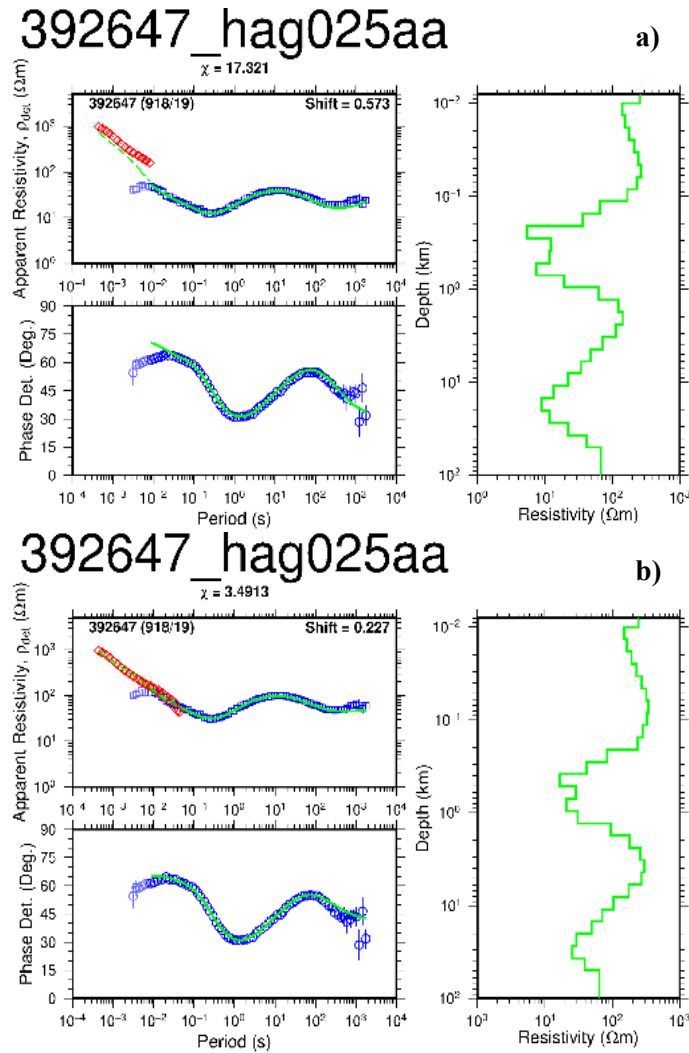


FIGURE 11: A typical result of 1D joint inversion of TEM and MT data from Hágöngur geothermal field. Red diamonds are measured TEM apparent resistivity, blue diamonds and blue circles are determinant of MT apparent resistivity and phase, respectively. Solid lines show the response of the resistivity model to the right. Shift multipliers used are shown in the upper right hand corners of the apparent resistivity panels. In a) the shift multiplier is 0.573 which is obviously an underestimate, not tying the different curves well together; while in b) it is 0.227, which provides a good fit to the combined TEM and MT data and the model response

The primary magnetic field transient creates eddy currents below the transmitter loop and as the initial near-surface eddy currents decay, they in turn induce eddy currents at greater depths. The rate of change of the secondary field, due to induced eddy currents, is measured using an induction coil. The depth of exploration that will be mapped in a vertical sounding configuration can vary from tens of metres to thousand metres, depending on the transmitter loop size and source current.

As shown in Figure 14 , the transmitter (Tx) transmits bipolar half-duty current, with equal current on and off segments and linear turn-off. The receiver (Rx) records the induced voltage at time gates equally distributed on log-scale during current off. In the central-loop configuration, the induced voltage is measured in a receiver coil at the centre of a circle transmitter loop as shown in Figure 14. The transmitter and the receiver need to be synchronised so that Rx knows when Tx starts to turn off. And also, Rx should know the time (T_{OFF}) it takes to turn off the current. The transient voltage induced decays with time after the current turn-off and is eventually drowned in noise.

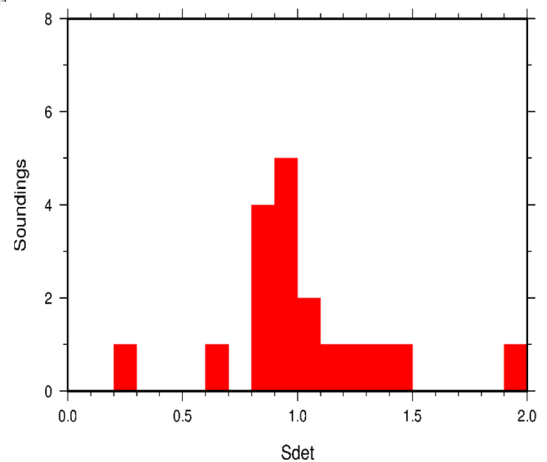


FIGURE 12: Static shift histogram for the Hágöngur high-temperature geothermal field

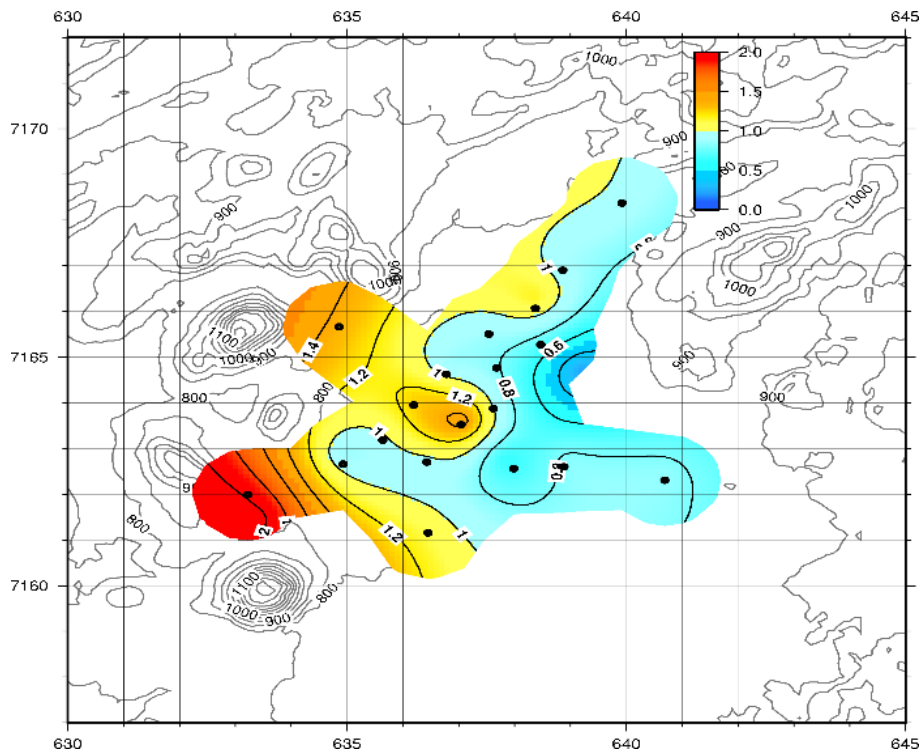


FIGURE 13: Static shift distribution map for Hågöngur, black dots are MT locations

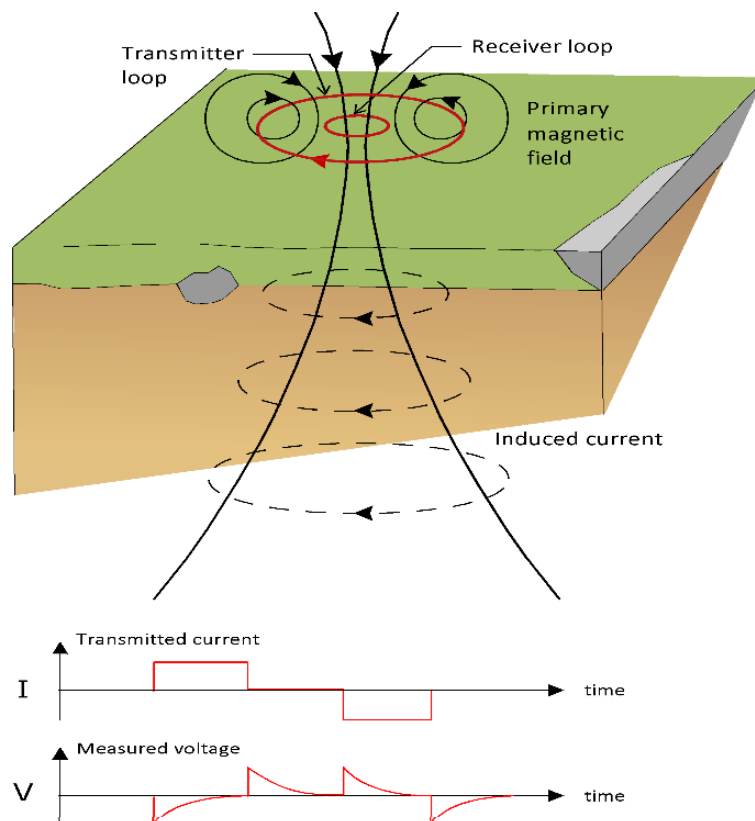


FIGURE 14: Set-up of a TEM sounding and the transient current flow in the ground (modified from Flóvenz et al., 2012)

The induced voltage $V(t,r)$ for a central-loop configuration on a homogeneous half space of conductivity σ is given by (Árnason, 1989):

$$V(t,r) = I_0 \frac{C(\mu_0 \sigma r^2)^{3/2}}{10\pi^{1/2} t^{5/2}} \quad (36)$$

where $C = A_r n_r A_s n_s \frac{\mu_0}{2\pi r^3}$;
 t = Elapsed time after the transmitter current is turned off (s);
 r = Radius of the transmitter loop (m);
 A_r = Cross-sectional area of the receiver coil (m²);
 n_r = Number of windings in the receiver coil;
 μ_0 = Magnetic permeability in vacuum (H/m);
 A_s = Cross-sectional area of the transmitter loop (m²);
 n_s = Number of windings in the transmitter loop;
 I_0 = Transmitted current (A);
 $V_{t,r}$ = Measured voltage (V).

Equation 36 can be used to define apparent resistivity, $\rho_a(t)$, in terms of induced voltage after the source current is turned off, given by (Árnason, 1989) as:

$$\rho_a = \frac{\mu_0}{4\pi} \left(\frac{2\mu_0 I_0 A_r n_r A_s n_s}{5t^{5/2} V_{t,r}} \right)^{2/3} \quad (37)$$

3. PREVIOUS STUDY AT THE HÁGÖNGUR GEOTHERMAL AREA

3.1 Location and accessibility

Hágöngur high-temperature geothermal area is located in the central highlands within the active volcanic zone, a few kilometres west of the Vatnajökull glacier, in Iceland. This area is very remote. Access to the area is available by using the Sprengisandur highland road, from a mountain track heading towards Vonarskard with an elevation of about 800 m a.s.l.

3.2 Geology

The Hágöngur area has been explored by Landsvirkjun (The National Power Company of Iceland). Geological investigations have been done occasionally in the area between the glaciers Vatnajökull and Hofsjökull. The geology of the Hágöngur is little known except that is being confined to the northern margin of the eastern volcanic zone with abundance of exposed Pleistocene and Holocene volcanics. Jóhannesson and Saemundsson (2003) have presumed that the area is an independent central volcano, but it has also been proposed that the Hágöngur area is in direct relation and a part of an elongated central volcano from Tungnafellsjökull in the northeast, extending southwards to the Hágöngur geothermal area (Fridleifsson et al., 1996). In this area, all exposed volcanic formations have a normal magnetization and as a result they are younger than 700,000 years (Piper, 1979). The area is in many ways quite unique in comparison with other high-temperature geothermal area in Iceland. It is entirely buried in glacio-fluvial sediments, supposedly filling an old lake basin.

3.3 Geophysics

In April 1998, a transient electromagnetic (TEM) survey was carried out in the Hágöngur area in order to get reliable data on the size and thermal conditions of the geothermal system. The TEM survey

revealed a high-resistivity core of about 28 km² at 1000 m depth approximately. Including the low-resistivity cap surrounding the high-resistivity core, the size of the high-temperature area is about 50 km², comparable to the resistivity depicted at the same level in the Krafla high-temperature area in Northern Iceland (Karlsdóttir, 2000). The resistivity anomaly at sea level is shown in Figure 15 with the low-resistivity cap and high-resistivity core mentioned separately.

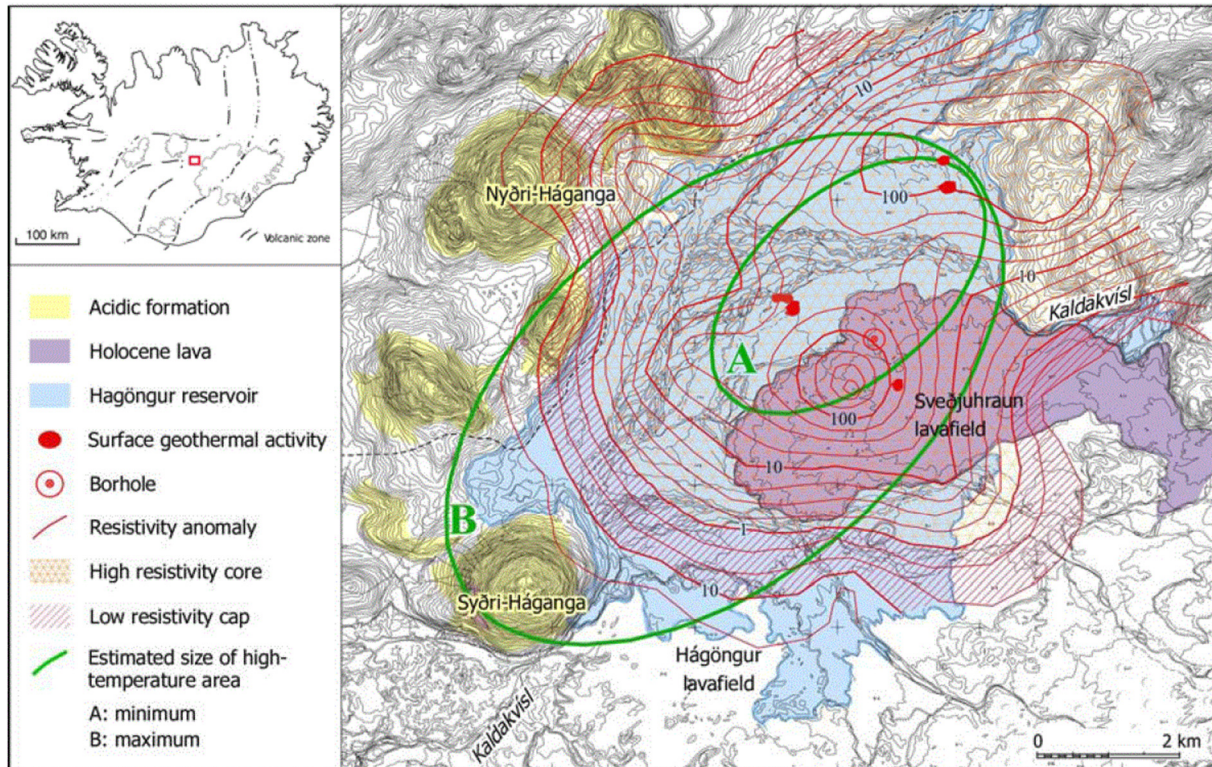


FIGURE 15: Location of the Hágöngur geothermal area and a simplified geological map with the resistivity anomaly (from Karlsdóttir, 2000) in the area at sea level

3.4 Lithology in well HG-01

An exploration well HG-01, the first deep exploration well drilled in the Hágöngur geothermal field, is located above the centre of the high-resistivity core. The well was drilled to a total depth of 2360 m in 2002. The lithology in this well and distribution of alteration minerals from analysis of drill cuttings are simplified in Figure 16.

4. MT AND TEM SURVEY AT HÁGÖNGUR HIGH-TEMPERATURE GEOTHERMAL FIELD

4.1 The location of the MT and TEM measurements

The main aim of this study was to learn about the application of MT and TEM measurements. Data from Hágöngur geothermal field were used for that purpose. The location of MT and TEM soundings in Hágöngur used in this report and the associated resistivity profiles are given in Figure 17. The data were measured by ÍSOR's staff and are used here with the permission of Landsvirkjun (The National Power Company of Iceland). Nineteen MT soundings and eighteen TEM soundings were performed on three profiles. Two of them trend SW-NE direction and the third one SE-NW. The resistivity data and its interpretation are presented in a separate Appendices report (Ali Soumail, 2015).

4.2 Data acquisition and processing

MT data acquisition. For an MT sounding, the equipments needed are data logger, two pairs of electric dipoles and three magnetic sensors. Generally, the data logger has 5 channels, 3 for the orthogonal horizontal and vertical magnetic field (H_x, H_y, H_z), and 2 for the orthogonal horizontal electric field (E_x, E_y). The data logger can control the acquisition process, amplify and filter the data, and convert them to digital format for storage.

The distance between the electrodes of the dipoles is usually in the range of 50-100 m. The measurement of the magnetic fields is made by a magnetic field sensor – coils are oriented in the x, y and z direction. The electric field is determined as $E_i = U/D_i$ where U is the voltage and D_i is the distance between a pair of electrodes in the direction of $i = x, y$.

A spirit level and compass are used in the MT set up to align the measurement axes in such a way that the x, y directions are horizontal and orthogonal to each other and the z direction is vertical. Generally, x positive direction is taken as magnetic North, y positive direction as magnetic East and z positive direction as vertical downwards. After Fourier transforming the recorded time series data are obtained in the frequency range of 300 - 0.001 Hz

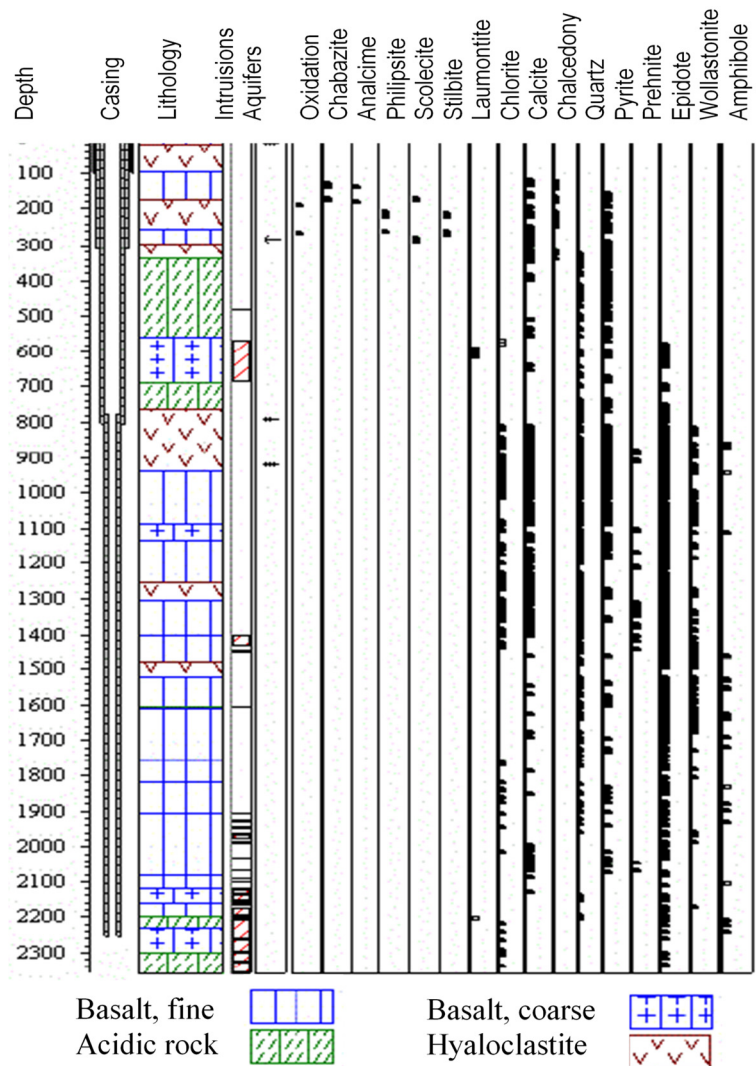


FIGURE 16: Simplified lithology in well HG-01 and distribution of alteration minerals from analysis of drill cuttings (Jónsson et al., 2005)

TEM data acquisition. For a TEM sounding, the instruments needed are generator, receiver, receiver coil(s), a current transmitter and wire for the transmitter loop. The description below applies to the PROTEM-67 system from Geonics, Ltd. At the measurement site, the first thing to do is to turn on the equipments and heat the crystals used for synchronization. Then the receiver and the transmitter are connected by a cable and the crystallizing synchronized. Usually, the set-up uses a square transmitter loop, 100 m to 300 m each side. A current of about 15-20 A is transmitted into the loop. A prism is used to make the loop as rectangular as possible by determining the right angle directions. The receiver coils are laid down in the centre of the transmitter loop.

After laying out the loops, the power source is started, the current and the turn off time in the transmitter are recorded in the data book. At low frequency (2.5 Hz), the current is measured to get a more stable value, and at high frequency (25 Hz), the turn off time is measured. The current and turn off time values are recorded into the receiver. Repeated measurements are done for different gains and stacking, first at

low frequency and then at high frequency. Low-frequency measurements are performed with a large receiver loop and a smaller standard receiver coil. The high-frequency measurements are made only with the small receiver coil.

4.3 1D inversion of resistivity data at Hágöngur area

4.3.1 TEM data processing and 1D interpretation

The raw TEM data were processed by the programme TemX developed by Árnason (2006b). This program enables visual editing of the raw data to remove outliers and unreliable data points before stacking over repeated measurements and calculating late time apparent resistivity as a function of time. 1D inversion of TEM is achieved by software called TEMTD which is a Linux/UNIX program (Árnason, 2006a). This software assumes that the source loop is a square and that the receiver coil/loop is at the centre of the source loop. The current waveform is also assumed to have equal current-on and current-off time segments. The transient response is calculated both as induced voltage and late time apparent resistivity as function of time. All the TEM soundings in the Hágöngur field have been interpreted by 1D inversion. The inversion was done by the Occam inversion as will be seen later in this report. In 1D inversion it is assumed that the earth consists of horizontal layers with different resistivity and thickness. The 1D interpretation determines the layered model whose response can best fit the measured responses (an example is seen in Figure 18). The remaining TEM soundings and models are given in Appendix I (Ali Soumail, 2015).

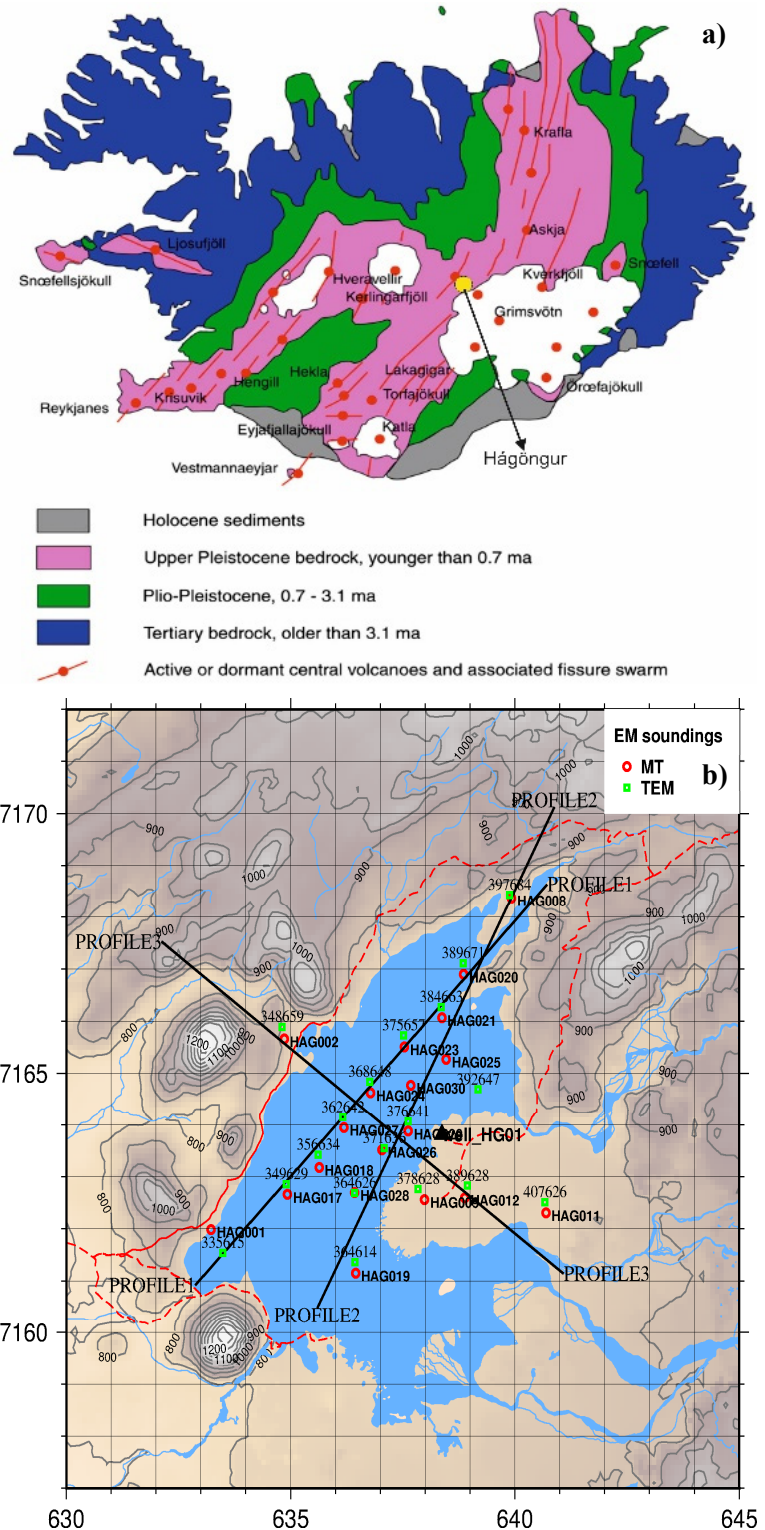


FIGURE 17: Location of the Hágöngur geothermal area (a) and the MT/TEM stations and the resistivity profiles (b). The red circles are the MT stations, the green squares are the TEM soundings, the black triangle is well HG-01 and red lines are roads

4.3.2 MT data processing and 1D interpretation

The processing of the collected time series data recorded from the MT equipment starts by using the time series viewer option in the SSMT2000 software (Phoenix Geophysics, 2005). It gives a first indication of the data quality that influences decision making on whether to repeat the sounding or not. Then parameter files (tbl) are edited to reflect the setup for the collected data. The resulting time series are Fourier transformed to the frequency domain, and then the different auto- and cross-powers are calculated using the robust processing method (RPM). The data are graphically edited using MTeditor, a Phoenix geophysics software, by masking the outliers to achieve apparent resistivity and phase curves as shown in Figure 19. The resulting MT parameters are all saved as EDI files.

The spectral EDI files from MTeditor are further processed through dos2unix which changes the edi-files from window based environment to a Linux readable format so that the commands spect2edi can calculate various parameters and can give the results in the standard format EDI making these ready to be used for inversion. Some of these programmes were developed at ISOR such as spect2edi. Finally, the inversion will be done through the TEMTD programme. The data were also run through another programme edi2ps to generate PostScript graphs. And finally ps2raster transforms the postscript files to PNG, which is the case of the pictures in this report. The plots in Figure 20 show an example of processed MT data. The remaining processed MT data are given in Appendix II (Ali Soumail, 2015).

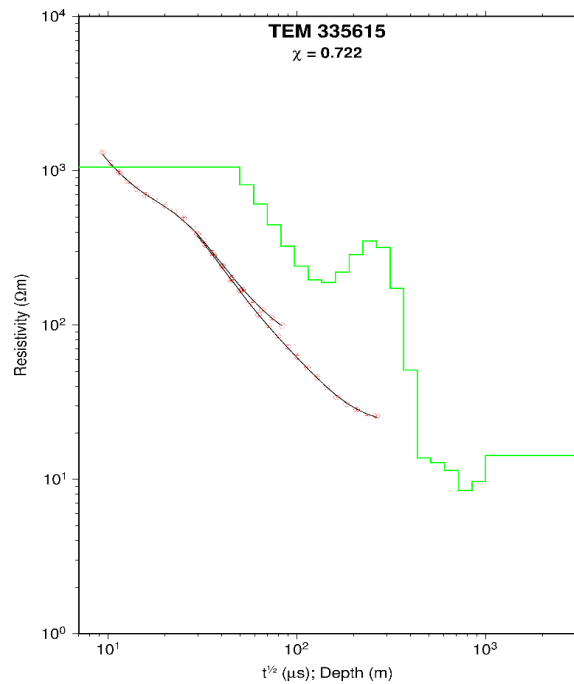


FIGURE 18: 1D inversion results from the TEM sounding 335615; the red dots are the calculated apparent resistivity points from voltage data; the green line shows the layered model generated by TEMTD; the black line is the response from the model

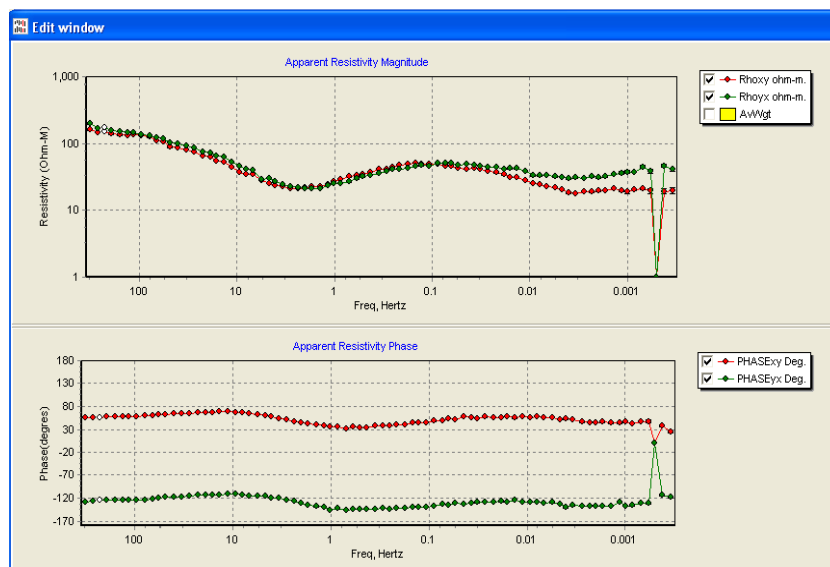


FIGURE 19: MTeditor output showing the apparent resistivity and phase curves of Hágöngur sounding HAG011

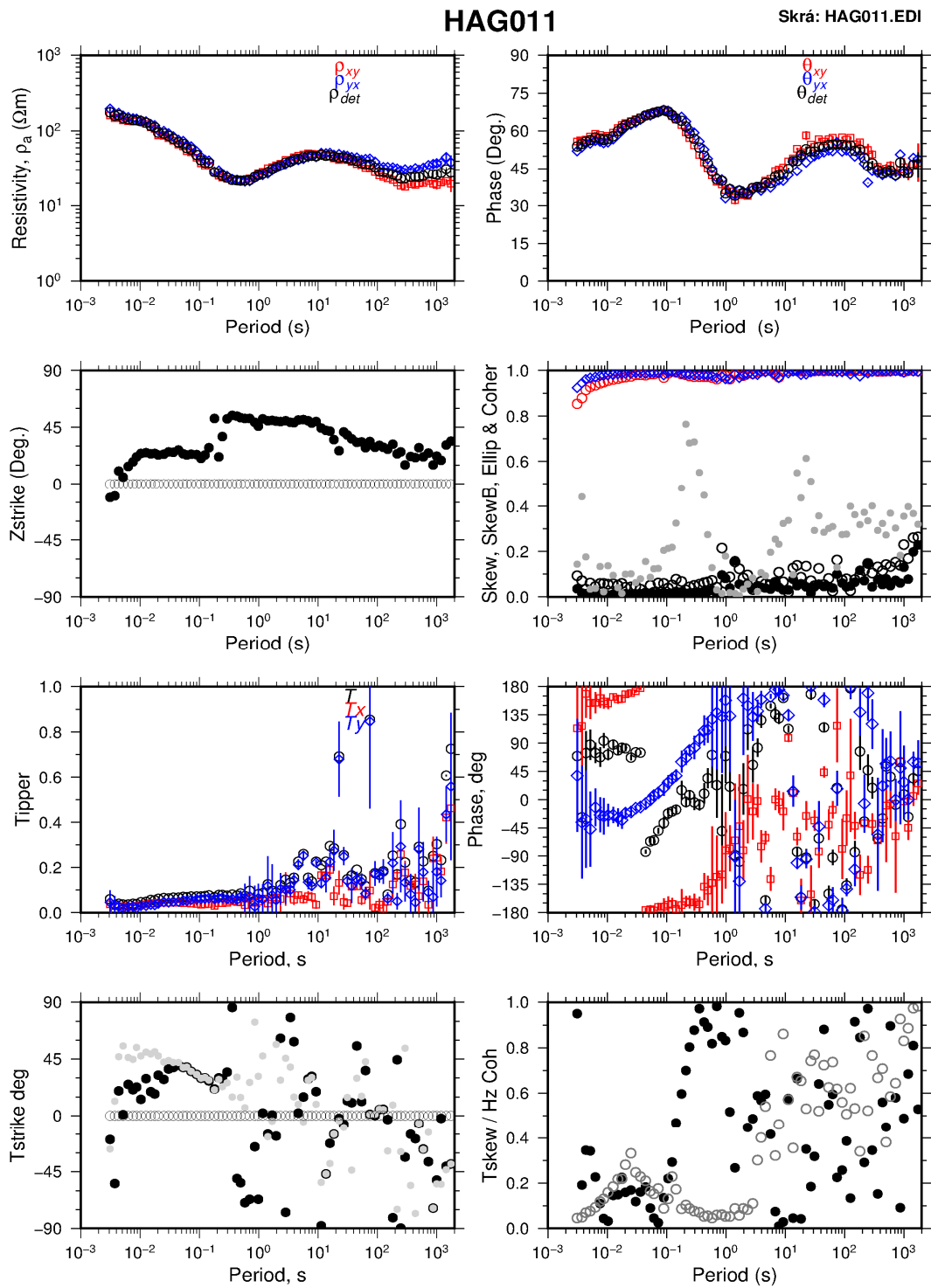


FIGURE 20: Processed MT data for sounding HAG011 from Hágöngur geothermal field; the plots show the apparent resistivity and phase derived from the xy (red) and yx (blue) components of the impedance tensor and the determinant invariant (black), the Z-strike or Swift angle (black dots), and multiple coherency of xy (red) and yx (blue), and skew (black dots) and ellipticity (grey dots). The lowermost four graphs show different representations of the Tipper values

4.3.3 1D joint inversion of MT and TEM

All data were inverted using Occam inversion method with varying first and second order derivatives of the resistivity layers such that the model will be optimized for resistivity smoothness and avoid unnecessary oscillations in their values. The 1D inversion was done with TEMTD. An example is given in Figure 21. The remaining 1D joint inversion soundings are given in Appendix III (Ali Soumail, 2015).

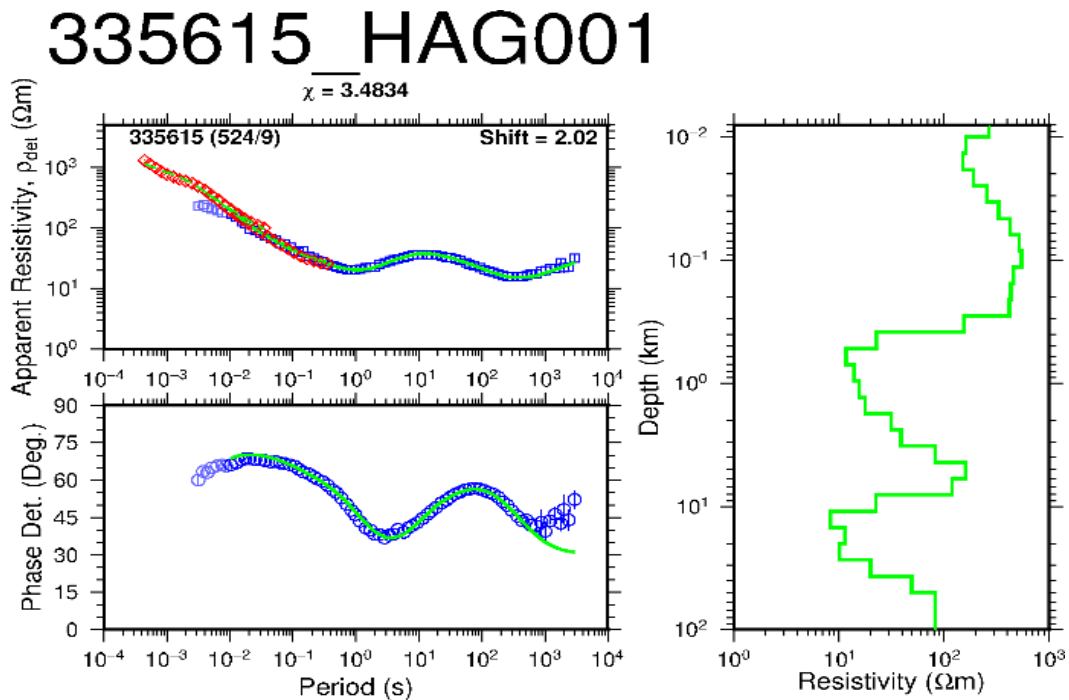


FIGURE 21: Results for joint 1D inversion of TEM and MT data. Red diamonds: TEM apparent resistivities transformed to a pseudo-MT curve; blue squares: measured apparent resistivities; blue circles: apparent phase derived from the determinant of MT impedance tensor; light blue symbols to the left of the green curve: data not used in the inversion; green lines model calculations; vertical blue lines: error bars. Right panel: results of the 1D resistivity inversion model, in the left panels its synthetic MT apparent resistivity and phase response. Number shown on the top of the figure: HAG001 is the name of the MT station and 335615 is the name of the TEM station. The numbers in parenthesis (524/9) indicates that the two stations were 524 m apart and their elevation difference was 9 m. The Chi square χ is 3.4834, and the shift is 2.02

5. INTERPRETATION AND RESULTS

5.1 Cross-sections

The resistivity cross-sections presented in this report were plotted from results acquired from 1D inversion by a programme developed at ÍSOR called TEMCROSS (Eysteinnsson, 1998). This programme calculates the best lines between the selected stations on a profile. Then it plots the resistivity isolines based on the 1D model generated for each sounding.

Three cross-sections were made in the Hágöngur area, as shown on the location map, see Figure 17. Two cross-sections (profile1 and profile2) are trending SW-NE and one (profile3) in SE-NW direction. All are presented in two versions, down to 2000 m b.s.l. and down to 10,000 m b.s.l.

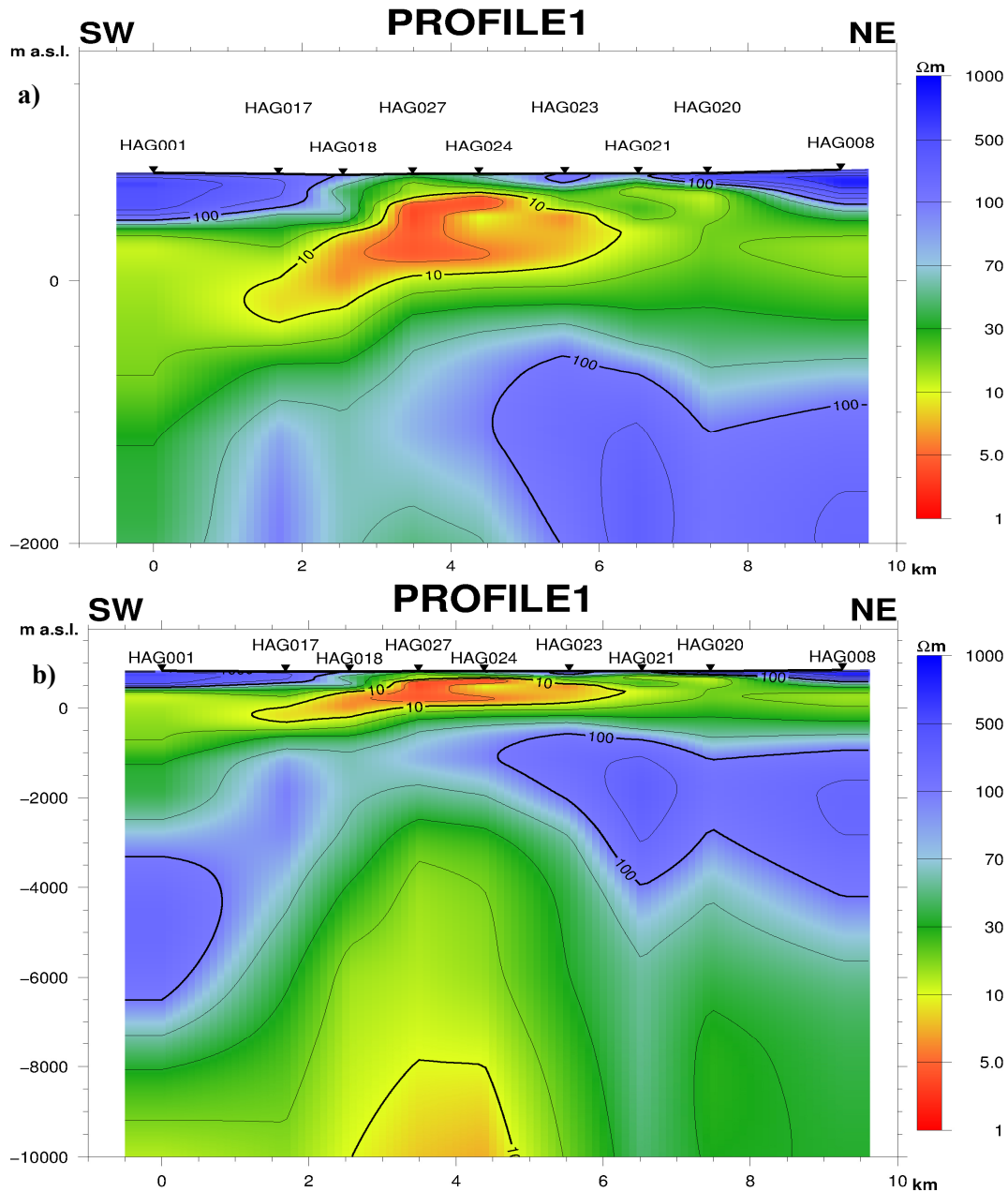


FIGURE 22: Resistivity cross-section profile 1; a) Down to 2000 m b.s.l.; b) Down to 10,000 m b.s.l.; the location of the profile is shown on Figure 17

Cross-section profile 1 (Figure 22) has 9 soundings and is about 9 km long. It shows a thin resistive layer near the surface which can be interpreted as unaltered basaltic lavas underlain by low-resistivity layer with resistivities less than 10 Ωm in the central part of the profile. This conductive layer, which lies roughly between 500 m a.s.l. and 500 m b.s.l., can be correlated with clay cap rocks such as smectite, zeolites or mixed-layer clays, indicating alteration temperatures somewhere between 100 and 220°C. Below this, a high-resistive layer is observed which may correspond to alteration zone with epidote,

chlorite. This indicates the presence of alteration temperatures above 250°C. This layer reaches down to 4-5000 m b.s.l. Further down lower resistivities are seen again.

Cross-section profile2 (Figure 23) has 6 soundings and is about 5 km long. This profile shows similar resistivity structures as the first one. But in addition to this, there is an indication of a fault trending NW-SE below -1000 m b.s.l.

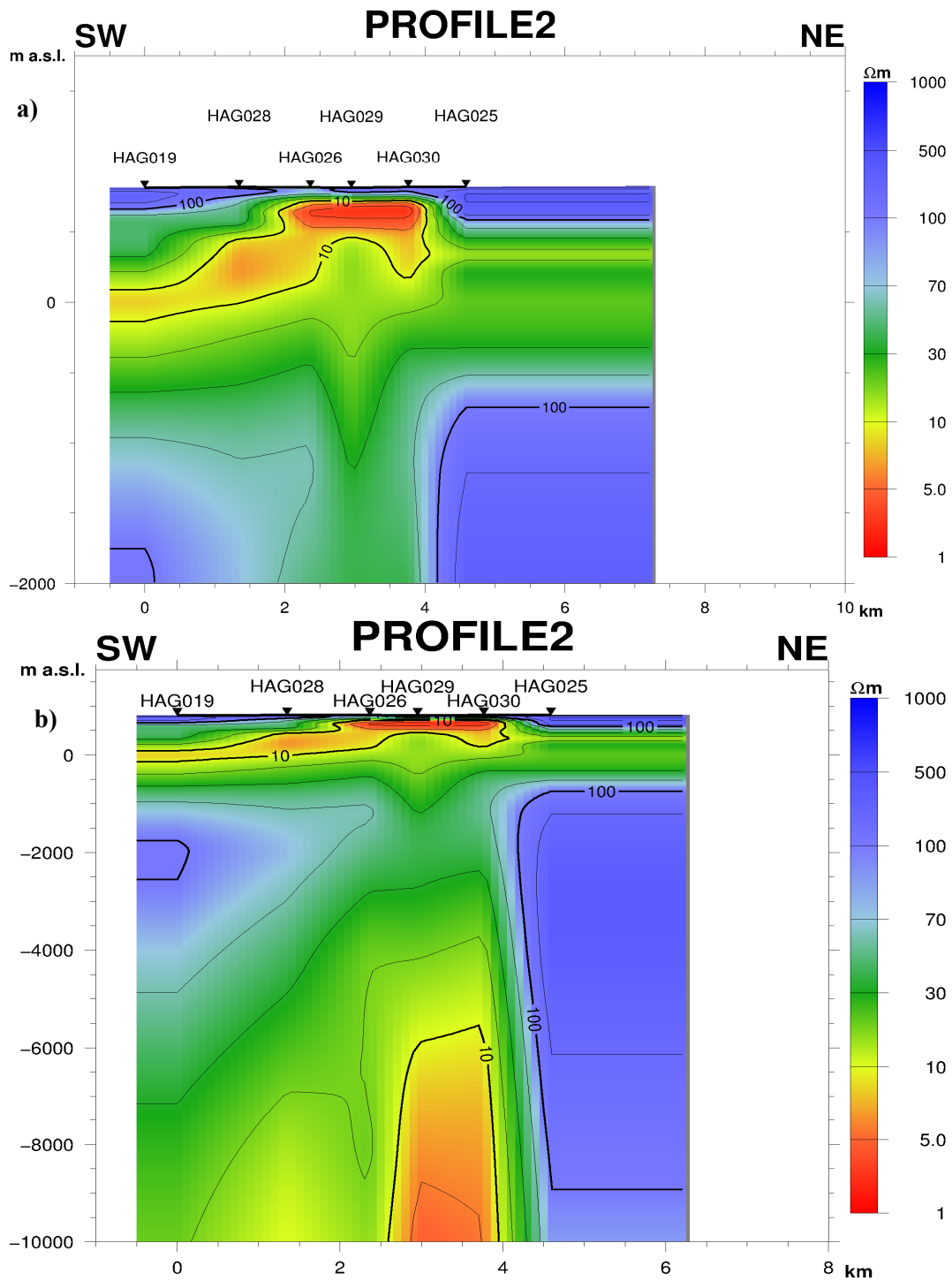


FIGURE 23: Resistivity cross-section profile2; a) Down to 2000 m b.s.l.; b) Down to 10,000 m b.s.l.

Cross-section profile3 (Figure 24) has 6 soundings and is about 7 km long. It shows the same resistivity structures. An upflow zone appears to be seen in this profile which trends from the deep conductive layer seen in soundings HAG26 and HAG24 which may correspond to the heat source.

A correlation between these profiles and well HG-01 drilled in this area has been found, and confirmed the assumptions on the different resistivity structures and the alteration minerals.

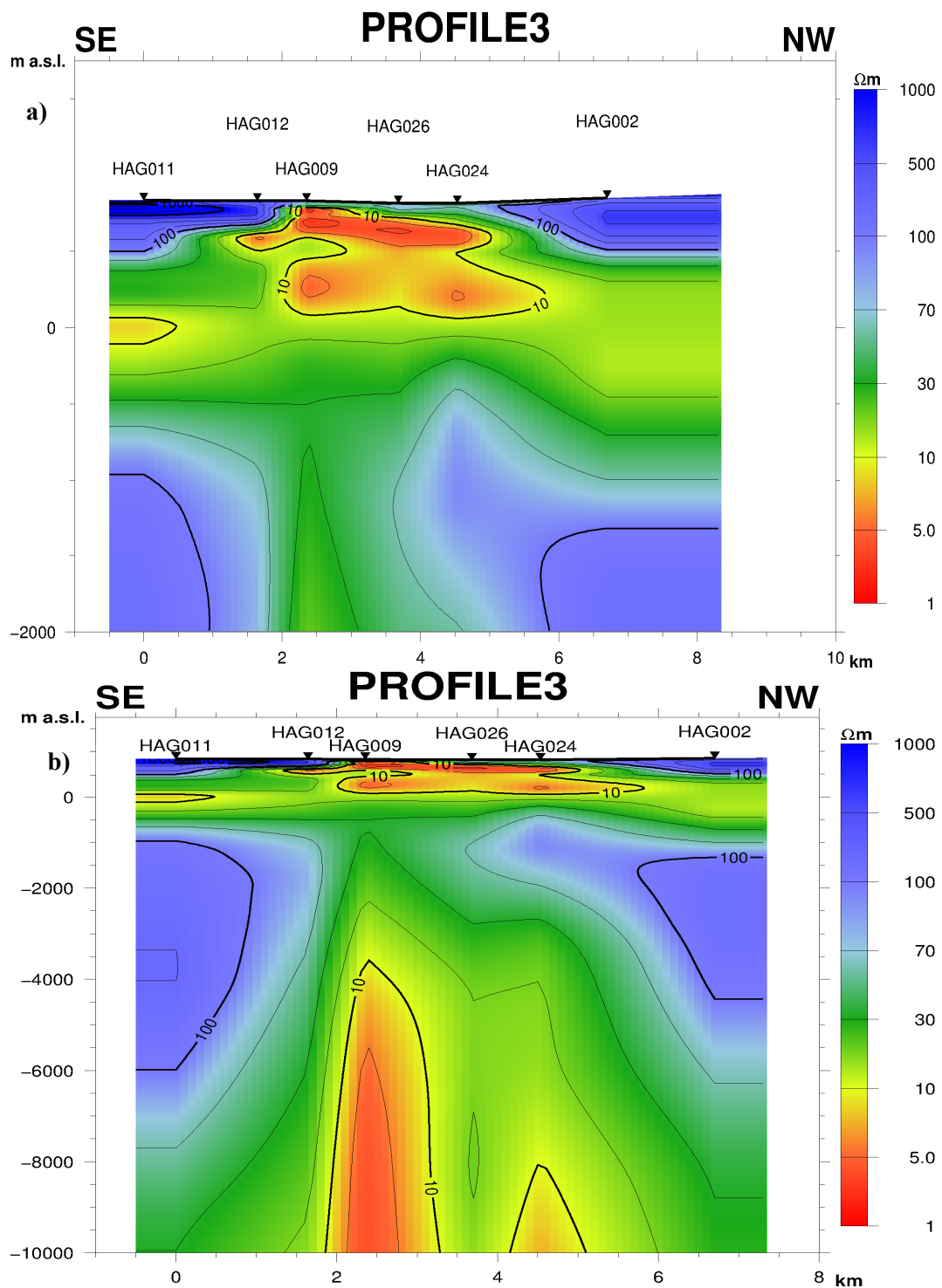


FIGURE 24: Resistivity cross-section profile3; a) Down to 2000 m b.s.l.; b) Down to 10,000 m b.s.l.

5.2 Iso-resistivity maps

Iso-resistivity maps using the TEMMAP program (Eysteinnsson, 1998) were made to display the resistivity at different depths in Hágöngur geothermal field. Several iso-resistivity maps were made, in this report four of them are displayed. However, it should be kept strictly in mind that the maps are based on relatively few soundings with non-uniform distribution.

Resistivity map at 800 m a.s.l. (Figure 25): The map shows a fairly uniform resistivity of about $100 \Omega\text{m}$ or slightly more, representing relatively unaltered rocks, except in the central part of the map, where the resistivity is about $30 \Omega\text{m}$.

Resistivity map at 400 m a.s.l. (Figure 26): A uniform conductive layer appears at this depth. It is more conductive in the centre part of the lake, with resistivities less than $10 \Omega\text{m}$. Else, it ranges between 10 and $30 \Omega\text{m}$. The conductive layer correlates with the clay cap rocks around the geothermal system.

Resistivity map at 1000 m b.s.l. (Figure 27): The map shows a fairly uniform layer with resistivities around $30 \Omega\text{m}$ at the centre to the southeast of the lake; outside this main area the resistivity is greater than $100 \Omega\text{m}$. The resistivities are probably controlled by high-temperature alteration minerals, dominated by epidote and chlorite, which could be the geothermal reservoir.

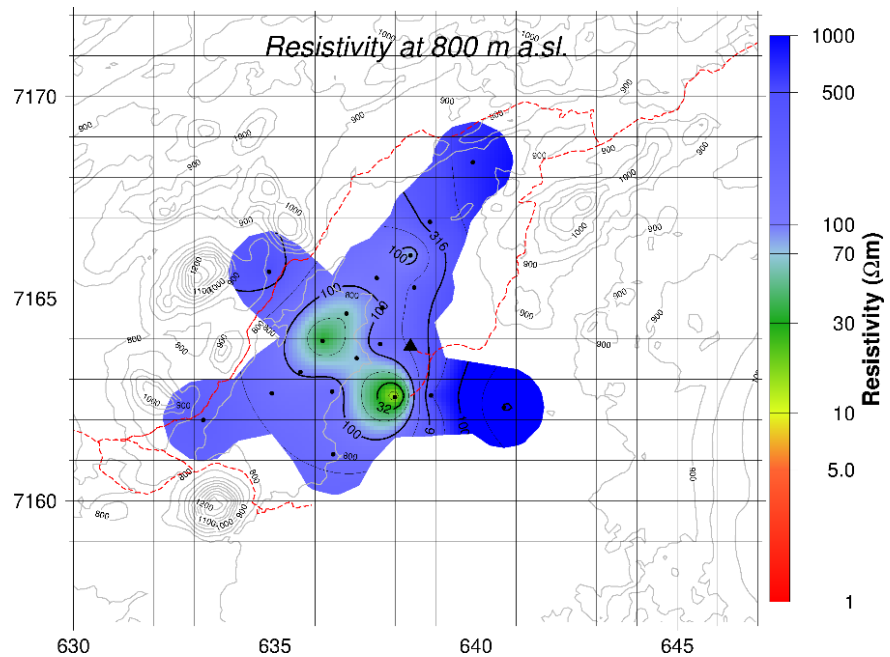


FIGURE 25: Iso-resistivity map at at 800 m a.s.l.; black dots denote MT soundings, the black triangle is well HG-01 and red lines are roads

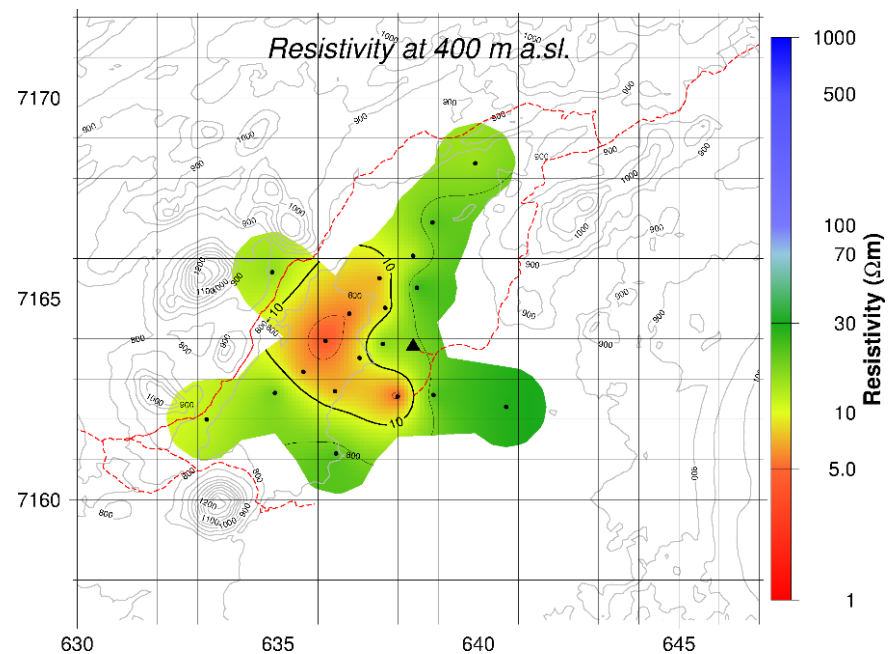


FIGURE 26: Iso-resistivity map at at 400 m a.s.l.; for figure legend, see Figure 25

Resistivity at 7500 m b.s.l. (Figure 28): At these deep levels the rocks are more conductive, specially in the centre of the lake, with resistivities less than 10 Ωm , but outside, they range between 10 and 30 Ωm . The conductive body might be associated with the heat source.

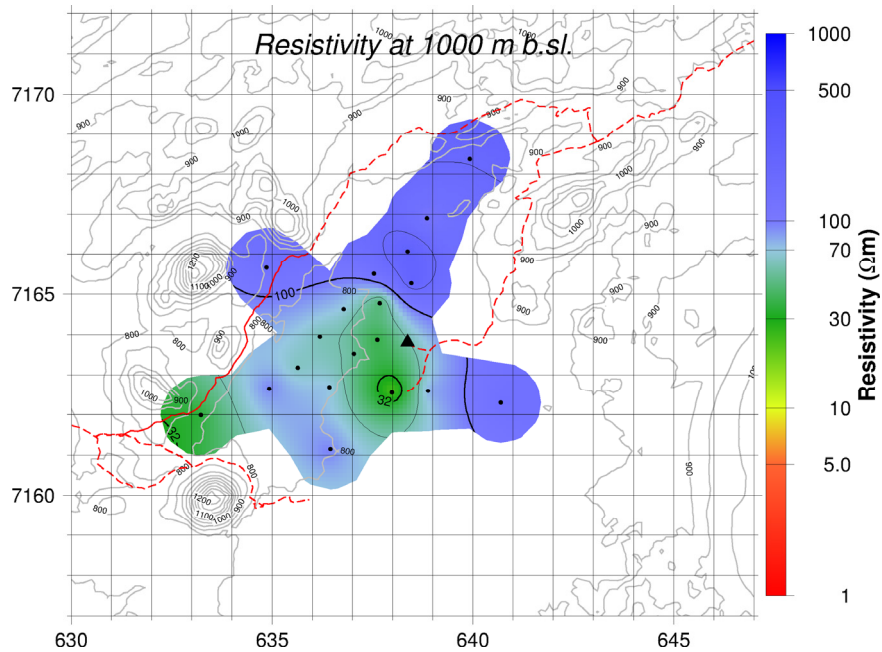


FIGURE 27: Iso-resistivity map at 1000 m b.s.l.; for figure legend, see Figure 25

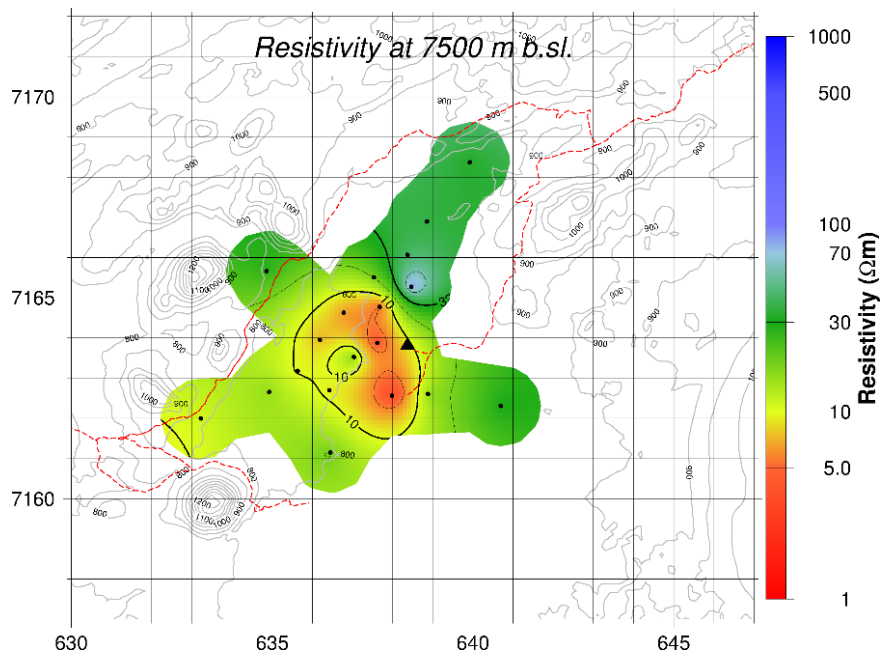


FIGURE 28: Iso-resistivity map at 7500 m b.s.l.; for figure legend, see Figure 25

5. CONCLUSIONS

According to the results of the resistivity survey in Hágöngur, as presented through 3 cross-sections and several iso-resistivity maps at different depths, and comparison with data from geothermal well HG-01, the area has a geothermal potential. The classical subsurface resistivity structures for geothermal systems in volcanic regions appears in the three profiles with high-low-high-low resistivity pattern. The following resistivity layers are displayed:

- High resistivity near surface caused by unaltered rocks;
- This is followed by low resistivity at around 400 m a.s.l. due to low-temperature alteration minerals, reaching down to about 1000 m b.s.l.,
- At 1000 m b.s.l. a resistive core is found similar to what can be expected from high-temperature alteration minerals in a high-temperature geothermal system.
- Finally, at 6-8 km depth there appears to be a deep conductor, which may be the heat source of Hágöngur geothermal system.

The centre of the geothermal reservoir seems to be localised between MT sounding HAG17 and HAG23 at levels below 900 m a.s.l. and there is an indication of a fault trending NW-SE below 1000 m b.s.l. An upflow zone can be seen in profile3 in the vicinity of resistivity stations HAG24 and HAG26.

These results of the resistivity structure of Hágöngur geothermal area show that the MT method is a powerful tool in mapping subsurface conductivity variations. It can investigate the electrical resistivity at great depth, even down to some tens of km, reveal geological faults and delineate the geothermal system. The joint inversion of MT/TEM is helpful in correcting static shift.

ACKNOWLEDGEMENTS

I would like to express my gratitude to the United Nations University Geothermal Training Programme (UNU-GTP) of Iceland for granting me the opportunity to be a fellow in this excellent programme and Landsvirkjun (National Power Company of Iceland) for providing the data. Many thanks go to director Mr. Lúdvík S.Georgsson, deputy director Mr. Ingimar G. Haraldsson, Ms. Thórhildur Ísberg, Ms. Málfrídur Ómarsdóttir and Mr. Markús A.G. Wilde, for their terrific support and facilitation of the training programme.

Special thanks to my supervisors, Mr. Gylfi Páll Hersir and Mr. Knútur Árnason for always being there for me and working with me full time during this research work. Furthermore, I wish to give my thanks to Mr. Arnar Már Vilhjálmsson for his assistance with my project. More thanks to my colleagues at UNU-GTP in Geophysical Exploration section for their fruitful discussions and sharing of knowledge. To the entire UNU Fellows of 2015, many thanks.

To my family, your support during these six months away was paramount. Most importantly, thanks to the Almighty Allah who taught mankind by the pen what they didn't know.

REFERENCES

Abdou, A.S., 2015: *Appendices to the report "TEM and MT resistivity surveying: Data acquisition, processing and 1D inversion with an example from Hágöngur geothermal field, Mid-Iceland"*. UNU-GTP, Iceland, report 6 appendices, 30 pp.

Archie, G.E., 1942: The electrical resistivity log as an aid in determining some reservoir characteristics. *Tran. AIME*, 146, 54-62.

- Árnason, K., 1989: *Central loop transient electromagnetic sounding over a horizontally layered earth*. Orkustofnun, Reykjavík, Iceland, report OS-89032/JHD-06, 129 pp.
- Árnason, K., Karlsdóttir, R., Eysteinnsson, H., Flóvenz, Ó. G., and Gudlaugsson, S.T., 2000: The resistivity structure of high-temperature geothermal systems in Iceland. *Proceedings of the World Geothermal Congress 2000, Kyushu-Tohoku, Japan*, 923-928.
- Árnason, K., 2006a: *TEM TD (Program for 1D inversion of central-loop TEM and MT data)*. ÍSOR-Iceland GeoSurvey, Reykjavík, Iceland, short manual, 16 pp.
- Árnason, K., 2006b: *TemX short manual*. ÍSOR-Iceland GeoSurvey, Reykjavík, internal report, 17 pp.
- Árnason K., Eysteinnsson, H., and Hersir, G.P., 2010: Joint 1D inversion of TEM and MT data and 3D inversion of MT data in the Hengill area, SW Iceland. *Geothermics*, 39, 13-34.
- Árnason, K., 2015: The static shift problem in MT Soundings. *Proceedings of the World Geothermal Congress 2015, Melbourne, Australia*, 12 pp.
- Badilla, E.D., 2011: Resistivity imaging of the Santa Maria sector and the northern zone of Las Pailas geothermal area, Costa Rica, using joint 1D inversion of TDEM and MT data. Report 8 in: *Geothermal training in Iceland 2011*. UNU-GTP, Iceland, 85-118.
- Cagniard, L., 1953: Basic theory of the magneto-telluric method of geophysical prospecting. *Geophysics*, 18, 605-635.
- Dakhnov, V.N., 1962: Geophysical well logging. The application of geophysical methods; electrical well logging. *Q. Colorado Sch. Mines*, 57-2, 445 pp.
- Eysteinnsson, H., 1998: *TEMMAP and TEMCROSS plotting programs*. ÍSOR – Iceland GeoSurvey, Reykjavík, unpublished programs and manuals.
- Flóvenz, Ó.G., Georgsson, L.S., and Árnason, K., 1985: Resistivity structure of the upper crust in Iceland, *J. Geophys. Res.*, 90, 10,136-10,150.
- Flóvenz, Ó.G., Spangerberg, E., Kulenkampff, J., Árnason, K., Karlsdóttir, R., Huenges, E., 2005: The role of electrical interface conduction in geothermal exploration. *Proceeding of the World Geothermal Congress 2005, Antalya, Turkey*, 9 pp.
- Flóvenz, Ó.G., Hersir, G.P., Saemundsson, K., Ármannsson, H., and Fridriksson Th., 2012: Geothermal energy exploration techniques. In: Sayigh, A. (ed.), *Comprehensive renewable energy, vol 7*. Elsevier Oxford, United Kingdom, 51-95.
- Fridleifsson, G.Ó., Ólafsson, M., and Bjarnason, J.Ö., 1996: *Geothermal activity in Köldukvislarbotnar*. Orkustofnun, Reykjavík, Iceland, report OS-96014/JHD-04 (in Icelandic), 32 pp.
- Henley, R.W. and Ellis, A.J., 1983: Geothermal systems, ancient and modern: A geochemical review. *Earth Sci. Reviews*, 19, 1-50.
- Hersir, G.P., and Björnsson, A., 1991: *Geophysical exploration for geothermal resources. Principles and applications*. UNU-GTP, Iceland, report 15, 94 pp.
- Hersir, G.P., and Árnason, K., 2009: Resistivity of rocks. *Paper presented at "Short Course on Surface Exploration for Geothermal Resources"*, organized by UNU-GTP and LaGeo, Santa Tecla, El Salvador, 8 pp.

Jóhannesson, H., and Saemundsson, K., 2003: *Active central volcanoes in Iceland*. ÍSOR, Reykjavík, Iceland, unpublished map (in Icelandic).

Jónsson, S.S., Gudmundsson, Á., and Pálsson, B., 2005: The Hágöngur high-temperature area, Central-Iceland. Surface exploration and drilling of the first borehole, lithology, alteration and geological setting. *Proceeding for the World Geothermal Congress 2005, Antalya, Turkey*, 6 pp.

Kaufman A.A., and Keller, G.V., 1983: *Frequency and transient sounding. Methods in geochemistry and geophysics, vol. 16*. Elsevier Scientific Publishing Co., Amsterdam, Netherlands, 685 pp.

Karlsdóttir, R., 2000: *The high-temperature area in Köldukvíslarbotnar. TEM-survey in 1998*. Orkustofnun, Reykjavík, Iceland, report OS-2000/060 (in Icelandic), 60 pp.

Keller, G.V., and Frischknecht, F.C., 1966: *Electrical methods in geophysical prospecting*. Pergamon Press Ltd., Oxford, United Kingdom, 527 pp.

Phoenix Geophysics, 2005: *Data processing. User guide's*. Phoenix Geophysics, Ltd., Toronto.

Piper, J.D.A., 1979: Outline of volcanic history of the region west of Vatnajökull, Central Iceland. *J. Volcanol. & Geothermal Res.*, 5, 87-98.

Quist, A.S., and Marshall, W.L., 1968: Electrical conductances of aqueous sodium chloride solutions from 0 to 800°C and at pressures to 4000 bars. *J. Phys. Chem.*, 72, 684-703.

Tikhonov, A.N., 1950: Determination of the electrical characteristics of the deeper strata of the earth's crust. *Dokl. Akad. Nauk*, 73, 295-297 (in Russian).